

Accepted Manuscript

Synthesis, X-ray structure of organometallic ruthenium (II) *p*-cymene complexes based on P- and N- donor ligands and their in vitro antibacterial and anticancer studies

Parichad Chuklin, Vachirawit Chalermpanapan, Thidarat Nookeaw, Saowanit Saithong, Kittipong Chainok, Saowalak Phongpaichit, Adisorn Rattanaphan, Nararak Leesakul

PII: S0022-328X(17)30412-6

DOI: [10.1016/j.jorganchem.2017.06.017](https://doi.org/10.1016/j.jorganchem.2017.06.017)

Reference: JOM 20004

To appear in: *Journal of Organometallic Chemistry*

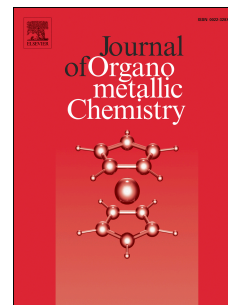
Received Date: 24 June 2016

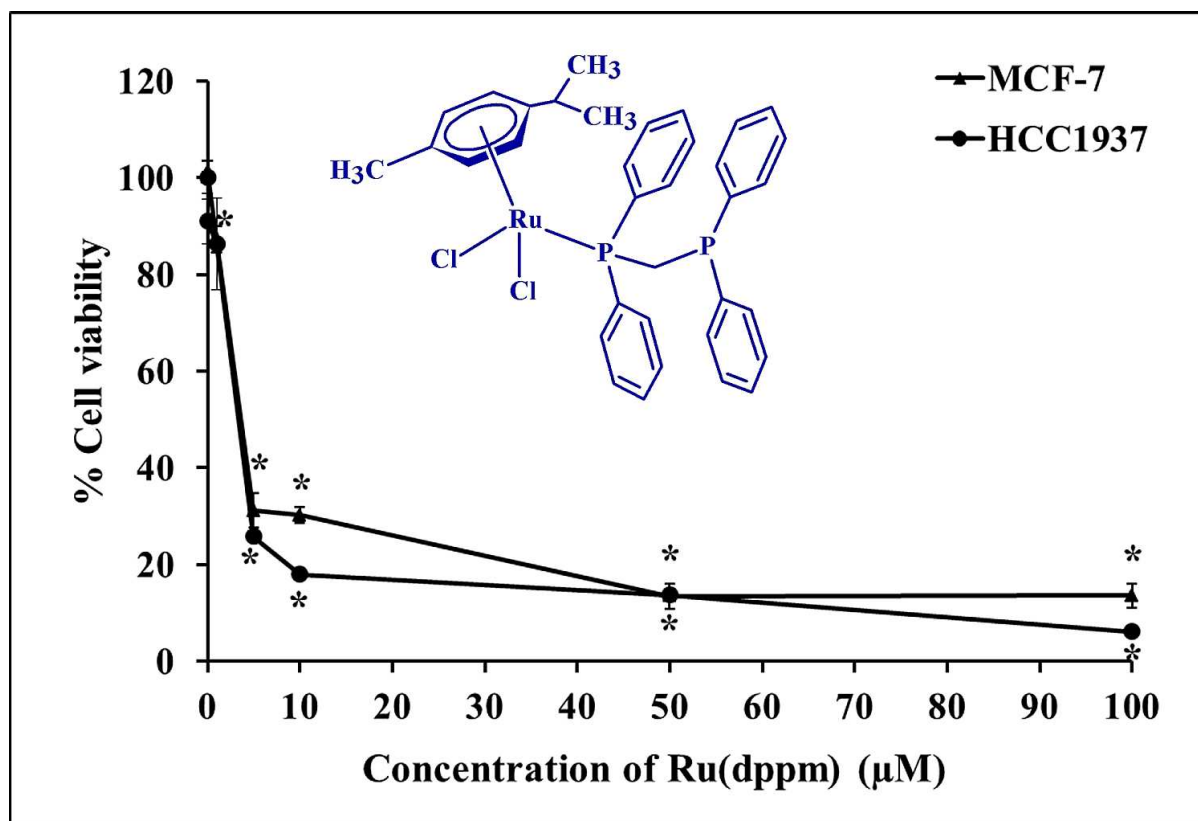
Revised Date: 10 June 2017

Accepted Date: 18 June 2017

Please cite this article as: P. Chuklin, V. Chalermpanapan, T. Nookeaw, S. Saithong, K. Chainok, S. Phongpaichit, A. Rattanaphan, N. Leesakul, Synthesis, X-ray structure of organometallic ruthenium (II) *p*-cymene complexes based on P- and N- donor ligands and their in vitro antibacterial and anticancer studies, *Journal of Organometallic Chemistry* (2017), doi: 10.1016/j.jorganchem.2017.06.017.

This is a PDF file of an unedited manuscript that has been accepted for publication. As a service to our customers we are providing this early version of the manuscript. The manuscript will undergo copyediting, typesetting, and review of the resulting proof before it is published in its final form. Please note that during the production process errors may be discovered which could affect the content, and all legal disclaimers that apply to the journal pertain.





Synthesis, X-ray structure of organometallic ruthenium (II) p-cymene complexes based on P- and N- donor ligands and their in vitro antibacterial and anticancer studies

Parichad Chuklin^a, Vachirawit Chalermpanapan^a, Thidarat Nookeaw^b, Saowanit Saithong^a, Kittipong Chainok^c, Saowalak Phongpaichit^d, Adisorn Rattanaphan^b, Nararak Leesakul^{a,*}

^aDepartment of Chemistry and Center for Innovation in Chemistry, Faculty of Science, Prince of Songkla University, Hat Yai, Songkhla 90110, Thailand

^b Department of Pharmaceutical Chemistry, Faculty of Pharmaceutical Sciences, Prince of Songkla University, Hat Yai, Songkhla 90110, Thailand

^cDepartment of Physics, Faculty of Science and Technology, Thammasat University, Klong Luang, Pathumthani, 12120 Thailand

^dNatural Products Research Center and Department of Microbiology, Faculty of Science, Prince of Songkla University, Hat Yai, Songkhla 90110, Thailand

Abstract

Two new arene compounds containing bis-diphosphinomethane (dppm) and *tert*-butylpyridine (tbp) ligands as important components in Ruthenium(II) complexes were synthesized and characterized by X-ray crystallography, and spectroscopy of ¹H-NMR, ¹³C-NMR, 2D-NMR, FTIR and CHN analysis. The synthesized complexes were evaluated in vitro as anticancer agents of human breast cancer cell lines, MCF-7 and HCC-1937, using the MTT assay. Both complexes showed an interesting behavior especially the compound of [Ru(*p*-cymene)(dppm)Cl₂]. It exhibited anticancer activity against both tested cell lines with greater IC₅₀ values than cisplatin against all breast cancer cells. Both MCF-7 and HCC1937 cells exhibited 16-fold sensitivity to the [Ru(*p*-cymene)(dppm)Cl₂] compared to cisplatin. Furthermore, the [Ru(*p*-

cymene)(dppm)Cl₂] complex significantly inhibited both *Staphylococcus aureus* ATCC25923 ,and MRSA = methicillin - resistant *Staphylococcus aureus* with MIC/MBC values of 8/200 $\mu\text{g. mL}^{-1}$ and 32/128 $\mu\text{g. mL}^{-1}$, respectively. In addition, it showed inhibition activity on *Cryptococcus neoformans* ATCC90113 flucytosine - resistant, CN90113, with an MIC/MBC value of 64/128 $\mu\text{g. mL}^{-1}$.

Keywords : antimicrobial activity, anticancer activity, Ru(II)-arene

Corresponding author : Tel.: 066 74 288421 (N. Leesakul), Fax.: 066 74 558841

E-mail addresses : nararak.le@psu.ac.th

1. Introduction

At the present time, some platinum drugs like *cis*-platin, carbo-platin and oxaliplatin are commonly used in the treatment of numerous types of cancer cells [1]. Nevertheless, these kinds of drugs can cause side effects including dehydration, risk of infection, kidney toxicity and many other abnormalities [2]. Half sandwich ruthenium(II)-arene complexes have been widely investigated and challenged to develop their pharmaceutical potential as anti-cancer agents with lower toxicity to normal cells than platinum(II) complexes. Half-sandwich metallocenes are effectively used for medicinal applications. Various half sandwich organometallic (η^6 -arene)-ruthenium (II) complexes with *p*-cymene ligands show promising anticancer behavior [3-4]. A distorted psuedo-tetrahedral structure coordinated with *p*-cymene to the ruthenium(II) center, like the typical “piano-stool” geometry, is of extensive interest. Other coordinated bonds normally occur with functional and chloro ligands. There exist several types of functional ligands with Nitrogen [5], Oxygen [6], Sulfur [7] and Phosphorus [8] donors. Most structures are designed to be ionic complexes soluble in water [9-10]. On the other hand, many neutral complexes exhibit promise as anticancer drugs [11-12] because they are kinetically stable, relatively lipophilic, and their metal atoms are in states of low oxidation [13]. Notable examples of anticancer compounds are ruthenium complexes consisting of diphosphine derivative ligands like 1,1-bis(diphenylphosphino) methane (dppm) and 4,5-bis(diphenylphosphino)-9,9-dimethylxanthene (Xantphos). Recently reported by Rodríguez-Bárzano and coworkers [14], they exhibited excellent IC50 values in nanomolar normoxic A2780 (human ovarian carcinoma) and HT-29 (human colon carcinoma) cell lines. Their reported complexes are both in the form of neutral and ionic structures of chelating bidentate diphosphine ligands. Nevertheless, no study has been carried out of the monodentate bonding of this kind of ligand.

Here we present the synthesis and structure determination, by single crystal X-ray diffraction and spectroscopic techniques, of half sandwich neutral complexes of organometallic Ru(II)-p-cymene with two different kinds of P and N-donor ligands of 1,1-bis(diphenyl phosphino)methane (dppm) and *tert*-butylpyridine (tbp), respectively. The complexes have general structures of [Ru(p-cymene)(L)Cl₂], where (L) = dppm and tbp and (p-cymene) = η^6 -p-cymene. As a consequence of their particular chemical structure, dichloro ligands are believed to display similar activity to the *cis*-dichloro motif of the well-established anticancer drug cisplatin. We investigated the ability of these two complexes to inhibit the growth of the breast cancer cell lines MCF-7 and HCC-1937, and also their anti-bacterial and anti-fungal activities. The [Ru(p-cymene)(dppm)Cl₂] complex is more encouraging than pyridine ligand and *cis*-Platin for the treatment of breast cancer.

2. Experimental Section

2.1 Materials

The chemicals of [RuCl(η^6 -p-cymene)(μ -Cl)]₂ were purchased from Merck, *tert*-butylpyridine (tbp) was obtained from Sigma-Aldrich. The tetrahydrofuran, diethyl ether and acetonitrile solvents were reagent grades from RCI Labscan and used as received without any further purification.

2.2 Instrumentation

The melting points were determined using a Thomas HOOVER, Unimelt 0-360 °C apparatus. FTIR spectra (KBr disk, 4000–400 cm⁻¹) were recorded with a BX PerkinElmer FTIR spectrophotometer. ¹H NMR data were measured using a CDCl₃ solvent with a Bruker

300 MHz NMR spectrometer. Tetramethylsilane (TMS) was used as an internal standard. The orange single crystal of $[\text{Ru}(\text{p-cymene})(\text{dppm})\text{Cl}_2]$ was obtained by recrystallization and the diffraction collected with a Bruker APEX-II CCD diffractometer with graphite-monochromated Mo $K\alpha$ radiation ($\lambda = 0.71073 \text{ \AA}$), 33925 reflections. The diffraction data were obtained by SMART, SAINT v8.34A and SADABS [15]. The structure was solved by ShelXS [16]. The anisotropic thermal parameters were refined to all non-hydrogen. All hydrogen atoms were placed in calculated, ideal positions and refined using a riding model. The *Olex2* [17], *WinGXv2014.1* [18] and *Mercury3.8* [19] programs were used to prepare the materials and molecular graphics for publication. Crystallographic data of $[\text{Ru}(\text{p-cymene})(\text{dppm})\text{Cl}_2]$ has been deposited at Cambridge Crystallographic Data Center via http://www.ccdc.cam.ac.uk/data_request/cif (or from the Cambridge Crystallographic Data Centre, 12 Union Road, Cambridge CB21EZ, U.K.; fax: +44 1223 336 033 or email deposit@ccdc.cam.ac.uk) with the CCDC1486230 and can be received upon request. The X-ray data are reported as supplementary crystallographic data.

2.3 Synthesis pathway

The complexes of $[\text{Ru}(\text{p-cymene})(\text{dppm})\text{Cl}_2]$ and $[\text{Ru}(\text{p-cymene})(\text{tbp})\text{Cl}_2]$ were synthesized in the same procedure. The starting material of $[\text{RuCl}(\text{p-cymene})(\mu\text{-Cl})_2]$ dimer (0.1837 g, 0.3 mmol) was dissolved in warm THF (15 mL) and stirred continuously for 1 hour. The dppm (0.192 g, 0.5 mmol) or tbp (0.2 mL, 1.2 mmol) ligands were slowly added to the warm (40°C) Ru(II) dimer solutions. Diethyl ether (5 mL) was added for precipitation. The solution was kept at room temperature for over one week. Orange precipitates of $[\text{Ru}(\text{p-cymene})(\text{dppm})\text{Cl}_2]$ and brownish-orange precipitates of $[\text{Ru}(\text{p-cymene})(\text{tbp})\text{Cl}_2]$ were obtained. The products were filtered and washed twice with diethyl ether and the synthesized complexes crystallized in a mixture of THF:ethylacetate (2:1 ratio) after a week. The

resulting crystals of [Ru(p-cymene)(dppm)Cl₂] were separated and dried under vacuum. The obtained complexes are readily soluble in DMSO.

2.3.1 Synthesis of [Ru(p-cymene)(dppm)Cl₂]

Yield : 69 %. Melting point: 178-180 °C. Anal Calcd for RuC₃₅H₃₆P₂Cl₂ (690.55): C, 60.87; H, 6.02. Found: C, 60.21; H, 6.22. IR: 2985 (νC-H), 1436 (νC=C), 1094 (νP-Ph), 800 (δC-H para disubstituted benzene), 708 (νP-C) cm⁻¹. ¹H NMR (300 MHz, CDCl₃) 12 signals: δ (ppm): 7.61 (dd, 4H, *J*_{HH} = 6.3 Hz), 7.21 (t, 2H, *J*_{HH} = 7.2 Hz), 7.10 (t, 4H, *J*_{HH} = 6.6 Hz), 5.15 (d, 2H, *J*_{HH} = 6.0 Hz), 4.90 (d, 2H, *J*_{HH} = 5.4 Hz), 4.60 (d, 4H, *J*_{HH} = 7.3 Hz), 3.75 (t, 4H, *J*_{HH} = 6.5 Hz), 2.47 (m, 4H, *J*_{HH} = 6.9 Hz), 1.91 (s, 3H), 1.85 (t, 2H, *J*_{HH} = 6.5 Hz), 1.71 (s, 2H), 0.94 (d, 6H, *J*_{HH} = 6.9 Hz).

2.3.2 Synthesis of [Ru(p-cymene)(tbp)Cl₂]

Yield : 61 %. Melting point: 178-180 °C. Anal Calcd for RuC₁₉H₂₆NCl₂ (690.55): C, 51.70; H, 6.17; N, 3.17. Found: C, 51.48; H, 6.28; N, 3.13. IR: 3073 (νC-H, aromatic ring), 2958 (νC-H, alkyl), 1617 (νC=C), 835 (δC-H para disubstituted benzene) cm⁻¹. ¹H NMR (300 MHz, CDCl₃) 8 signals: δ (ppm): 8.81 (d, 2H, *J*_{HH} = 6.3 Hz), 7.23 (d, 2H, *J*_{HH} = 7.2 Hz), 5.38 (d, 2H, *J*_{HH} = 6.0 Hz), 5.20 (d, 2H, *J*_{HH} = 5.4 Hz), 2.93 (m, 4H, *J*_{HH} = 6.9 Hz), 2.06 (s, 3H), 1.24 (d, 2H, *J*_{HH} = 6.5 Hz), 1.23 (s, 2H). ¹³C NMR (300 MHz, CDCl₃): 163, 115, 122, 103, 97, 83, 77, 35, 30, 27, 18 ppm. The ¹³C NMR spectrum was assigned on the basis of the proton-decoupled ¹³C and the HMQC, DEPT 135, DEPT 90 spectra (Supplementary data).

2.4 Antibacterial assay

All compounds were dissolved in dimethyl sulfoxide and tested against *Staphylococcus aureus* ATCC25923, a clinical isolate of methicillin-resistant *S. aureus*

(MRSA) SK1, and *Escherichia coli* ATCC25922 by a microdilution method involving a modification of Clinical and Laboratory Standards Institute (CLSI) M07-A9 [20]. The MICs are the lowest concentration of synthesized compounds with visible growth inhibition. Synthesized compounds of higher concentrations than the MIC, and the MIC were streaked onto a nutrient agar plate and incubated under appropriate conditions. The lowest concentration of compounds showing no growth was recorded as the MBC. Vancomycin and gentamicin were used as standard antibacterial agents for positive inhibitory controls.

2.5 Antifungal assay

The MICs of synthesized compounds were determined by a modification of the microbroth dilution CLSI M27-A3 [21] against yeast (*Cryptococcus neoformans* ATCC90113) and a modification of the microbroth dilution CLSI M38-A2 [22] against a clinical isolate of *Microsporium gypseum* MU-SH4. Microtiter plates were incubated at 35°C for 48 h for *C. neoformans*. The MFCs of the active compounds were determined by the streaking method on Sabouraud's dextrose agar. Amphotericin B was used as a positive inhibitory control for the yeasts.

2.6 Cell culture

Human breast adenocarcinoma cell lines, including MCF-7 (BRCA1 wild type, estrogen receptor (ER) positive) and HCC1937 (BRCA1 mutant, triple-negative breast cancer (TNBC)) were purchased from the American Type Culture Collections (ATCC, Rockville, MD). MCF-7 cells were grown in Dulbecco's modified eagle's medium (DMEM) without phenol red, while HCC1937 cells were grown in Roswell Park Memorial Institute 1640 medium (RPMI 1640) without phenol red. Both media were supplemented with 10% fetal bovine serum (FBS) and 1% penicillin-streptomycin. All cell lines were cultured at a constant temperature of 37°C in a 5% carbon dioxide (CO₂) humidified atmosphere.

2.7 In vitro cytotoxicity assay

The cytotoxic effect of both complexes on MCF-7 and HCC1937 cells was performed by the tetrazolium salt reduction (MTT) assay. Ten thousand cells were plated in each well of 96-well culture plates and grown at 37°C in 5% CO₂. After 24 h of seeding cells, the medium was removed and cells were treated with different concentrations of the two complexes. [Ru(*p*-cymene)(dppm)Cl₂] was dissolved in 1% DMSO at final concentrations of 0.01, 1, 5, 10, 50 and 100 µM and [Ru(*p*-cymene)(tbp)Cl₂] was dissolved in 1% DMSO at final concentrations of 100, 200, 500, 1000 and 2000 µM. The cells were then incubated at 37°C in 5% CO₂ for 48 h, after which each well was washed twice with 100 µl of phosphate buffered saline (PBS). Then 100 µl of 0.5 mg/ml of 3-[4,5-dimethylthiazol-2-yl]-2,5-diphenyltetrazolium bromide was added and the plates were further incubated at 37°C in 5% CO₂ for 4 h. Subsequently, the medium was removed and 200 µl of 100% DMSO was added to dissolve the purple formazan crystal. The absorbance of each well was determined spectrophotometrically at 570 nm. The percentage of cell viability was calculated as follows, % cell viability = (absorbance of the ruthenium complex treated cells)/(absorbance of the vehicle treated cells) x 100. The inhibiting concentration of each ruthenium complex that reduced the number of viable cells to 50% (IC₅₀) was derived by plotting log of the percentage cell viability versus concentration. Results were derived from four independent experiments each performed in at least triplicate.

Data are expressed as the standard error of the mean (\pm S.E.M.). Statistical analysis comparisons of the significant differences between the mean values was performed using one-way ANOVA. A probability of 0.01 or less was deemed statistically significant. The following notation is used throughout the manuscript: *, $p < 0.01$, relative to the control.

3. Results and Discussion

3.1 Synthesis and characterization

Two novel ruthenium(II) complexes $[\text{Ru}(\text{p-cymene})(\text{dppm})\text{Cl}_2]$ and $[\text{Ru}(\text{p-cymene})(\text{tbp})\text{Cl}_2]$ were synthesized by the reaction of $[\text{RuCl}(\text{p-cymene})(\mu\text{-Cl})_2]$ with the P and N donors of 1,1-bis(diphenylphosphino) methane and *tert*-butyl pyridine in tetrahydrofuran, respectively (scheme I).

<< Scheme I >>

The elemental analysis data of both complexes corresponded to the theoretically calculated values. The differences of C, H and N (in $[\text{Ru}(\text{tbp})(\text{p-cymene})\text{Cl}_2]$ complex) percentages between the calculated and experimental values deviate within 0.04-0.6 %. The FTIR spectra displayed some characteristic peaks in the 1600-700 cm^{-1} region (see supplementary data, S1). The $[\text{Ru}(\text{p-cymene})(\text{dppm})\text{Cl}_2]$ complex exhibited the stretching modes of P-C(Phenyl) at 520 cm^{-1} and 490 cm^{-1} corresponding to the frequencies reported by Jensen and Nielsen, 1963 [23]. P-C(alkyl) stretching frequencies appeared in the range of 700-1100 cm^{-1} . The $[\text{Ru}(\text{p-cymene})(\text{tbp})\text{Cl}_2]$ complex showed the stretching modes of C=C and C=N in the pyridine ring in the region of 1420-1620 cm^{-1} . Importantly, these peaks do not exist in the FTIR spectrum of the starting material, $[\text{RuCl}(\text{p-cymene})(\mu\text{-Cl})_2]$, which is evidence that the functional ligand coordinated with the Ru(II) center. The vibrational frequencies of C=C and C=N were compared with the free 4-*tert*-butylpyridine which are in the range of 1500-1700 cm^{-1} . A shift of *ca.* 100 cm^{-1} was observed. This red shifting frequency may be a result of the decrease of C=C and C=N bond order caused by π -backbonding from the d-orbital of Ru(II) to the π^* orbital of the pyridine moiety. Likewise, the C-P stretching mode of $[\text{Ru}(\text{p-cymene})(\text{dppm})\text{Cl}_2]$ is different from its free dppm ligand (1000 cm^{-1} [24]) for almost 500 cm^{-1} .

For $^1\text{H-NMR}$ spectra (see supplementary data, S2) of both complexes measured in CDCl_3 , the prospective resonances are detected for the (*p*-cymene) and the functional ligands of dppm and *tbp*. In consequence of the coordination of the functional ligands, downfield shifts of 0.15-0.25 ppm of the ligand ring protons are noticed in comparison with the free ligands. Likewise, downfield shifts were also found for the coordinated (*p*-cymene) in both complexes compared to the *p*-cymene ligand in $\text{RuCl}(\textit{p}\text{-cymene})(\mu\text{-Cl})_2$ complex. The chemical shifts are presented in the experimental section. The $^{13}\text{C-NMR}$ spectra (see supplementary data, S3) of $[\text{Ru}(\textit{p}\text{-cymene})(\textit{tbp})\text{Cl}_2]$ are in good agreement with the resonance signals of its structure.

The structure of the $[\text{Ru}(\textit{p}\text{-cymene})(\text{dppm})\text{Cl}_2]$ complex was determined by single crystal x-ray diffraction. Its molecular structure with atom numbering is displayed in Figure 1, selected bond lengths and angles are given in Table 1. The crystal structure of $[\text{Ru}(\textit{p}\text{-cymene})(\text{dppm})\text{Cl}_2]$ is a triclinic system with a *P*-1 space group. The mononuclear complex of Ru(II) is in four coordinations with π conjugated carbons in *cymene*, and in dppm through one of the phosphorus atoms and two chloro ligands show the piano-stool distorted psuedo-tetrahedral geometry. The Ru-C(*p*-cymene) lengths are between 2.161(4) and 2.235(3) Å; the average distance between Ru(II) and the centroid of the *p*-cymene ring is 1.6941(16) Å; and the average length of Ru-Cl is 2.4095(9) Å. All these measurements are similar to the relevant complexes in [25-26]. The length of Ru-P is 2.350(8) Å which is also close to the other compounds [27-28]. The bond angles around Ru(II) are in the range of $82.45(3)^\circ$ to $160.65(10)^\circ$. The largest angle can be observed in the C(2)-Ru-P(1). It is probably due to the steric bulk of the phosphinomethane groups. In the molecular structure, intramolecular π - π stacking is observed of the two opposed phenyl rings in the dppm ligand. The centroid-centroid distance is 3.955(3) Å as shown in Figure 2. In addition, there is intermolecular π - π stacking of two dppm phenyl rings and π - π stacking between the *cymene* and dppm phenyl

rings of two alternate adjacent molecules (Figure 2). This stabilizes the crystal packing with a centroid-centroid (Cg5---Cg5) distance of 4.328(3) Å. The π - π stacking between the cymene ring (Cg1) and the phenyl ring (Cg2) of dppm, Cg1----Cg2 stabilizes at 4.460(2) Å.

In addition, the intermolecular contacts in the packing were studied by Hirshfeld surface analysis. The Crystal Explorer program (Wolff et al., 2012) [31] was used to generate Hirshfeld surfaces mapped over d_{norm} . The mapping of d_{norm} was used to analyze the intermolecular contact distances, d_i and d_e , from the Hirshfeld surfaces between the nearest atom inside and outside molecules, respectively. Hirshfeld surfaces mapped over d_{norm} , shown in Figure 3, reveal a pair of hydrogen-bonds representing acceptors on the surfaces and they are shown as bright-red spots at Cl1 of C2-H2---Cl1(#1) and at Cl2 of C3-H3---Cl2(#1) with distances of 3.725(4) and 3.529(4) Å, respectively (for symmetry operation #1 : -x,1-y,1-z). Two-dimensional fingerprint plots (Rohl et al., 2008) [32] are shown in Figure 4 as the combination of d_e and d_i and provide a summary of intermolecular contacts in the crystal. The overall two-dimensional fingerprint plot is depicted in Fig. 4a, and those for the contacts of H---H, H---Cl/Cl---H, C---H/H---C are shown in Fig 4b-d. The greatest contribution to the overall Hirshfeld surface, i.e. 72.8%, is provided by H---H contacts in crystal packing. The contribution of 9.9 % from the H---Cl/Cl---H contacts corresponds to the C---H---Cl interactions, which are represented by a pair of asymmetric spikes at $d_e + d_i$ ca 3.2 Å (Fig. 4c). The asymmetrical peaks of the delineated finger print plot of Figure 4d, indicate C---H/H---C contacts with 14.3%, $d_e + d_i$ ca 3.6 Å, representing π - π stacking interactions in crystal packing.

<< Table 1 >>

<<Figure 1>>

<<Figure 2>>

<<Figure 3>>

<<Figure 4>>

3.2 Absorption

The absorption spectra of the [Ru(p-cymene)(dppm)Cl₂] and [Ru(p-cymene)(tbp)Cl₂] complexes (Figure 5) in chloroform were measured in the range of 200-800 nm. The absorption bands of [Ru(p-cymene)(dppm)Cl₂] and [Ru(p-cymene)(tbp)Cl₂] complexes in the visible region appear at the maximum wavelengths of absorption at 397 nm and 420 nm, respectively, providing low molar extinction coefficients ($< 1,700 \text{ M}^{-1}\text{cm}^{-1}$) which are ascribed to d-d transition of Ru(II). In contrast, π - π^* transition with high molar extinction coefficients ($> 10,000 \text{ M}^{-1}\text{cm}^{-1}$) is to be found in the non-visible UV region.

<<Figure 5>>

3.3 Antimicrobial activity of the [Ru(p-cymene)(dppm)Cl₂] and [Ru(p-cymene)(tbp)Cl₂] complexes

Using the agar microdilution method, we tested the antimicrobial activity of the two studied compounds against three types of bacteria, namely *S. aureus* (SA), methicillin - resistant *S. aureus* (MRSA) and *E. coli* ATCC25922 (EC). Growth inhibition was compared with that of the antibacterial drugs, vancomycin and gentamicin. In addition, we measured the antifungal activity of the complexes against one type of yeast (*C. neoformans* ATCC 90113). A comparison of these results with those produced by the standard antifungal drug amphotericin B is presented in Table 2. No activity was found from checking against each tested organism.

The [Ru(p-cymene)(dppm)Cl₂] complex shows antibacterial activities at concentrations < 32 μg. mL⁻¹. However, the [Ru(p-cymene)(tbp)Cl₂] complex does not exhibit such activities in the studied system. The results imply that the dppm ligand may have a strong influence on the bacterial growth inhibition mechanism not shown by the free ligand. The [Ru(p-cymene)(dppm)Cl₂] complex significantly inhibited *Staphylococcus aureus* ATCC25923, MRSA = methicillin - resistant *Staphylococcus aureus* with MIC/MBC values of 8/200 and 32/128 μg. mL⁻¹, respectively. The variation in the antimicrobial activity of the free ligand and the different metal complexes against the different microorganisms is due either to the differences in the ribosomes in the microbial cells or the impermeability of the microbe cells. It is worth noting that chelation is able to increase the ability of the complexes to permeate the microorganism cell membranes by decreasing the polarizability of the metal, as explained by Tweedy's chelation theory [23]. The [Ru(p-cymene)(dppm)Cl₂] has a more lipophilic structure than that of the [Ru(p-cymene)(tbp)Cl₂] due to the extra phenyl rings in the diphosphinomethane group. Penetration through the cell walls of bacteria is, therefore, much more possible than it is with the [Ru(p-cymene)(tbp)Cl₂] complex, leading to greater inhibition of bacterial growth.

The data obtained from the experiments suggested that the [Ru(p-cymene)(dppm)Cl₂] compound exhibits mild to good antifungal activity. Interestingly, the compound was more effective against bacteria than against fungi.

<< Table 2 >>

3.4 Anticancer activity

The antiproliferative property of the new ruthenium(II)arene complexes, [Ru(p-cymene)(dppm)Cl₂] and [Ru(p-cymene)(tbp)Cl₂] were tested in two different human breast cancer cells using the MTT assay. The percentage of cell viability was assessed as shown in

Figure 4 and 5. As can be seen in Figure 6, for each type of breast cancer cell, the observed cell growth inhibitory effect of $[\text{Ru}(\text{p-cymene})(\text{dppm})\text{Cl}_2]$ varied at similar concentrations. The same results for the $[\text{Ru}(\text{p-cymene})(\text{tbp})\text{Cl}_2]$ complex show clear differences at concentrations from 100 μM to 1000 μM , and no variation at concentrations from 1000 μM to 2000 μM . Representative results showed that the percentage cell viability of both breast cancer cells decreased as concentrations of $[\text{Ru}(\text{p-cymene})(\text{dppm})\text{Cl}_2]$ and $[\text{Ru}(\text{p-cymene})(\text{tbp})\text{Cl}_2]$ increased. The cytotoxic activities of the ruthenium complexes, compared to cisplatin, were determined as the IC_{50} values and are summarized in Table 3. Both ruthenium complexes can inhibit breast cancer cell growth, but with different cellular responses. Interestingly, $[\text{Ru}(\text{p-cymene})(\text{dppm})\text{Cl}_2]$ exhibited significantly greater cytotoxicity than $[\text{Ru}(\text{p-cymene})(\text{tbp})\text{Cl}_2]$ against cells of both cisplatin-resistant MCF-7 and cisplatin-sensitive, BRCA1-defective HCC1937.

A feature of the antiproliferative activity studies was tested as chemotherapeutic agents candidates for both cisplatin-resistant, BRCA1-competent MCF-7 and cisplatin-sensitive, BRCA1-deficient, triple-negative HCC1937 cells by the two ruthenium(II) arene complexes with different ligands, $[\text{Ru}(\text{p-cymene})(\text{dppm})\text{Cl}_2]$ and $[\text{Ru}(\text{p-cymene})(\text{tbp})\text{Cl}_2]$ as shown in Figure 6, 7 and Table 3. Both ruthenium complexes exerted cytotoxicity against both breast cancer cells in a concentration-dependent manner. It was of interest that the cytotoxicity of $[\text{Ru}(\text{p-cymene})(\text{dppm})\text{Cl}_2]$ was clearly greater than that of cisplatin or $[\text{Ru}(\text{p-cymene})(\text{tbp})\text{Cl}_2]$ against all breast cancer cells. Both MCF-7 and HCC1937 cells were 16 times more sensitive to the $[\text{Ru}(\text{p-cymene})(\text{dppm})\text{Cl}_2]$ than to cisplatin. Compared to cisplatin, $[\text{Ru}(\text{p-cymene})(\text{tbp})\text{Cl}_2]$ was less cytotoxic to the same cells by factors of 15 and 16 respectively. Compared to $[\text{Ru}(\text{p-cymene})(\text{dppm})\text{Cl}_2]$, it was respectively 247 and 275 times less cytotoxic. The greater cytotoxicity of $[\text{Ru}(\text{p-cymene})(\text{dppm})\text{Cl}_2]$ may be attributed to the larger size and surface area of its structure and the effect that has on the activity of the

coordinated diphenylphosphino ligand. The hydrophobicity of the complex, and its π -extended system could also be associated with its superior uptake into breast cancer cells [24.] These results agree very well with a previous study which showed that ruthenium(II) complexes containing 1,1'-bis(diphenylphosphino) ferrocene (dppf) exerted an enhanced anticancer activity against S-180 murine ascetic sarcoma 180, DU145 human prostate carcinoma, K562 chronic myeloid leukemia and A549 human lung carcinoma [25]. It was also interesting that HCC1937, known to be a BRCA1-defective (5382insC mutation) cell line lacking an estrogen receptor (ER), was significantly more sensitive than the BRCA1-competent MCF-7 cell line. Ruthenium sensitivity in the BRCA1-mutated cells might be related to dysfunctional BRCA1 that is unable to repair DNA damage induced by [Ru(p-cymene)(dppm)Cl₂] treatment, ultimately leading to breast cancer cell death [26-29]. However, the precise molecular mechanisms of action of this ruthenium(II)-arene complex remain largely unexplored and are of great interest for further investigation. Our results are the first evidence of the anticancer activity of [Ru(p-cymene)(dppm)Cl₂] against both cisplatin-resistant and BRCA1-defective breast cancer cells. Therefore, the ruthenium(II) arene complex containing diphenylphosphino ligand could be a promising therapeutic ruthenium-based agent for breast cancers.

<< Table 3 >>

<<Figure 6>>

<<Figure 7>>

4. Conclusion

The structures of half sandwich $[\text{Ru}(\text{p-cymene})(\text{dppm})\text{Cl}_2]$ and $[\text{Ru}(\text{p-cymene})(\text{dppm})\text{Cl}_2]$ complexes are pseudo-tetrahedral distorted geometry. The $[\text{Ru}(\text{p-cymene})(\text{dppm})\text{Cl}_2]$ complex presents as a promising powerful anticancer against MCF-7 and HCC1937 breast cell lines with a lower IC_{50} than that of cisplatin, while $[\text{Ru}(\text{p-cymene})(\text{tbp})\text{Cl}_2]$ shows much lower activity. It is favored by the diphosphine ligand more than the pyridine moiety. Although the mechanism of the inhibition of growth in cancer cells is not yet well understood, the binding of synthesized ruthenium complexes to DNA cancer cells is the main reason for their anticancer effect. Chloro ligands are labile which can cause further hydrolysis and allow Ru(II) to attach to base pairs of DNA cancer cells. The $[\text{Ru}(\text{p-cymene})(\text{dppm})\text{Cl}_2]$ exhibits moderate to good activity against SA and MRSA bacteria but only weak inhibition of CN yeast growth.

Acknowledgement

NL acknowledges financial support from the Prince of Songkla University under contract number (SCI560355S) as well as Center for Innovation in Chemistry (PERCH-CIC), the Commission on Higher Education and the Ministry of Education and Faculty of Science, PSU. AR thanks the National Research Council of Thailand and Prince of Songkla University (PHA570058S, PHA580500S and PHA580926S) for financial support. We would also like to thank Mr. Thomas Duncan Coyne for assistance with the English.

References

1. A. Kumar, A. Kumar, R. K. Gupta, R. P. Paitandi, K. B. Singh, S. K. Trigun, M. S. Hundal, D. S. Pandey, J. Organomet. Chem. 801 (2016) 68–79.

2. J. Q. Wang, P. Y. Zhang, L. N. Ji, H. Chao, *J. Inorg. Chem.* 146 (2015) 89-96.
3. S. Thangavel, M. Paulpandi, H. B. Friedrich, K. Murugan, S. Kalva, A. A. Skelton, J. *Inorg. Biochem.* 159 (2016) 50-61.
4. C. S. Allardyce, J. D. Paul, J. E. David, A. S. Paul, S. Rosario, *J. Organomet. Chem.* 668 (2003) 35-42.
5. G-S. Sanja, I. Ivanka, R. Gordana, T. Nina, Gl. Nevenka, R. Siniša, B. A. Vladimir, K. K. Bernhard, Lj. T. Živoslav, *Med. Chem.* 45 (2010) 1051-1058.
6. K. Wolfgang, G. H. Christian, A. N. Alexey, L. K. Maxim, O. J. Roland, B. Caroline, A. J. Michael, B. A. Vladimir, K. K. Bernhard, *Organomet.* 28 (2009) 4249-4251.
7. B. Floyd, D. Deidra, S. Jr. a. Michael, D. Jacob, Th. Jeffrey, W. Jason, C. Vernon, G. Nikolay, G-S. Antonio, P. S. Navindra, *J. Inorg. Biochem.* 105 (2011) 1019-1029.
8. A. V. Carsten, K. R. Anna, S. Rosario, J. Lucienne, J. D. Paul, *Eur. J. Inorg. Chem.* (2008) 1661-1671.
9. L. Bíró, D. Hüse, A. Cs. Bényei, P. Buglyó, *J. Inorg. Biochem.* 116 (2012) 116-125.
10. A. K. Renfrew, A. E. Egger, R. Scopelliti, C. G. Hartinger, P. J. Dyson, *Comptes Rendus Chimie.* 13 (2010) 1144-1150.
11. C. Scolaro, C. G. Hartinger, C. S. Allardyce, B. K. Keppler, P. J. Dyson, *J. Inorg. Biochem.* 102 (2008) 1743-1748.
12. X. Shang, T. F. S. Silva, L. M. D. R. S. Martins, Q. Li, M. F. C. Guedes da Silva, M. L. Kuznetsov, A. J. L. Pombeiro, *J. Organomet. Chem.* 730 (2013) 137-143.
13. G. Gasser, I. Ott, N. M.-Nolte, *J. Med. Chem.* 54 (2011) 3-25.

14. A. R.-Bárzano, R. M. Lord, A. M. Basri, R. M. Phillips, A. J. Blacker, P. C. McGowan, Dalton Trans. 44 (2015) 3265-3270.
15. Bruker (2013). SMART, SAINT and SADABS. Bruker AXS Inc., Madison, Wisconsin, USA.
16. O. V. Dolomanov, L. J. Bourhis, R. J. Gildea, J. A. K. Howard, H. Puschmann, J. Appl. Cryst. 42 (2009) 339-341.
17. G. M. Sheldrick, Acta Cryst. A71 (2015) 3–8.
18. L. J. Farrugia, J. Appl. Cryst. 45 (2012), 849–854.
19. C. F. Macrae, I. J. Bruno, J. A. Chisholm, P. R. Edgington, P. McCabe, E. R.-M. Pidcock, L. Rodriguez-Monge, R. Taylor, J. van de Streek and P. A. Wood, J. Appl. Cryst. 41 (2008). 466–470.
20. Clinical and Laboratory Standards Institute (CLSI) Methods for dilution antimicrobial susceptibility tests for bacteria that grow aerobically; approved standard- Ninth edition. CLSI document M07–A9. CLSI, Wayne (2012).
21. Clinical and Laboratory Standards Institute (CLSI). Reference method for broth dilution antifungal susceptibility testing of yeasts; approved standard-Third edition. CLSI documents M27–A3. CLSI, Wayne (2008a).
22. Clinical and Laboratory Standards Institute (CLSI). Reference method for broth dilution antifungal susceptibility testing of filamentous fungi; approved standard- Second edition. CLSI documents M38-A2. CLSI, Wayne (2008b).
23. K. A. Jensen and P. H. Nielsen, Acta Chim. Scand. 17 (1963) 1875-1885.
24. H.-G. Horn and K. Sommer, Spectrochim. Acta. 27A (1971) 1049-1054.

25. D. Schleicher, A. Tronnier, H. Leopold, H. Borrmann, T. Strassner, Dalton Trans. 45 (2016) 3260-3263.
26. H. Rosana, K. Jakob, K. Wolfgang, R. Urska, T. Boris, G. H.Christian, K. K. Bernhard, M. Damijan, T. Iztok, Organomet. 31 (2012) 5867-5874.
27. A. V. Carsten, K. R. Anna, S. Rosario, J. Lucienne, J. D. Paul, Eur. J. Inorg. Chem. (2008) 1661-1671.
28. S. K. Wolff, D. J. Grimwood, J. J. Mckinnon, M. J. Turner, D. Jayatilaka, M. A. Spackman, Crystal Explorer. The University of Western Australia (2012).
29. A. L. Rohl, M. Moret, W. Kaminsky, K. Claborn, J. J. Mckinnon, B. Kahr, Cryst. Growth &Des. 8 (2008) 4517-4525.
30. M. Muthukumar, P. Viswanathamurthi, Spectrochim. Acta Part A. (74) 2009 454-462.
31. S. Das, S. R. Sinha, K. Britto, A. G. Somasundaram Samuelson, J. Inorg. Biochem. 104 (2010) 93-104.
32. F. C. Pereira, B. A. Lima, A. P. de Lima, W. C. Pires, T. Monteiro, L. F. Magalhães, W. Costa, A. E. Graminha, A. A. Batista, J. Ellena, E. P. Siveira-Lacerda, J. Inorg. Biochem. 162 (2015) 87-92.
33. E. Alli, V. B. Sharma, A. R. Hartman, P. S. Lin, L. McPherson, J. M. Ford, BMC Pharmacol. (2011) 11-17.
34. R. M. Neve, K. Chin, J. Fridlyand, J. Yeh, F.L. Baehner, T. Fevr, L. Clark, N. Bayani, J. P. Coppe, F. Tong, T. Speed, P. T. Spellman, S. DeVries, A. Lapuk, N. J. Wang, W. LinKuo, J. L. Stilwell, D. Pinkel, D. G. Albertson, F. M. Waldman, F. McCormick, R. B. Dickson, M. D. Johnson, M. Lippman, S. Ethier, A. Gazdar, J. W. Gray, Cancer Cell. 10 (2006) 515-527.

35. P. Tassone, M. T. Di Martino, M. Ventura, A. Pietragalla, I. Cucinotto, T. Calimeri, A. Bulotta, P. Neri, M. Caraglia, P. Tagliaferri, *Cancer Biol Ther.* 8 (2009) 648-653.
36. T. Nhugeaw, P. Temboot, K. Hansongnern, A. Ratanaphan, *BMC Cancer.* 14 (2014) 73.

ACCEPTED MANUSCRIPT

Table 1 Selected bond lengths (Å) and bond angles (°) of [Ru(p-cymene)(dppm)Cl₂] complex

Ru(1)-P(1)	2.3500(8)
Ru(1)-ring centroid	1.6941(16)
Ru(1)-Cl(1)	2.4150(9)
Ru(1)-Cl(2)	2.4040(9)
P(1)-C(11)	1.825(3)
P(1)-C(17)	1.823(4)
P(1)-Ru(1)-Cl(1)	87.85(3)
P(1)-Ru(1)-Cl(2)	88.78(3)

Table 2. Antimicrobial activity levels of [Ru(p-cymene)(dppm)Cl₂] and [Ru(p-cymene)(tbp)Cl₂] complexes and starting materials in dmsO.

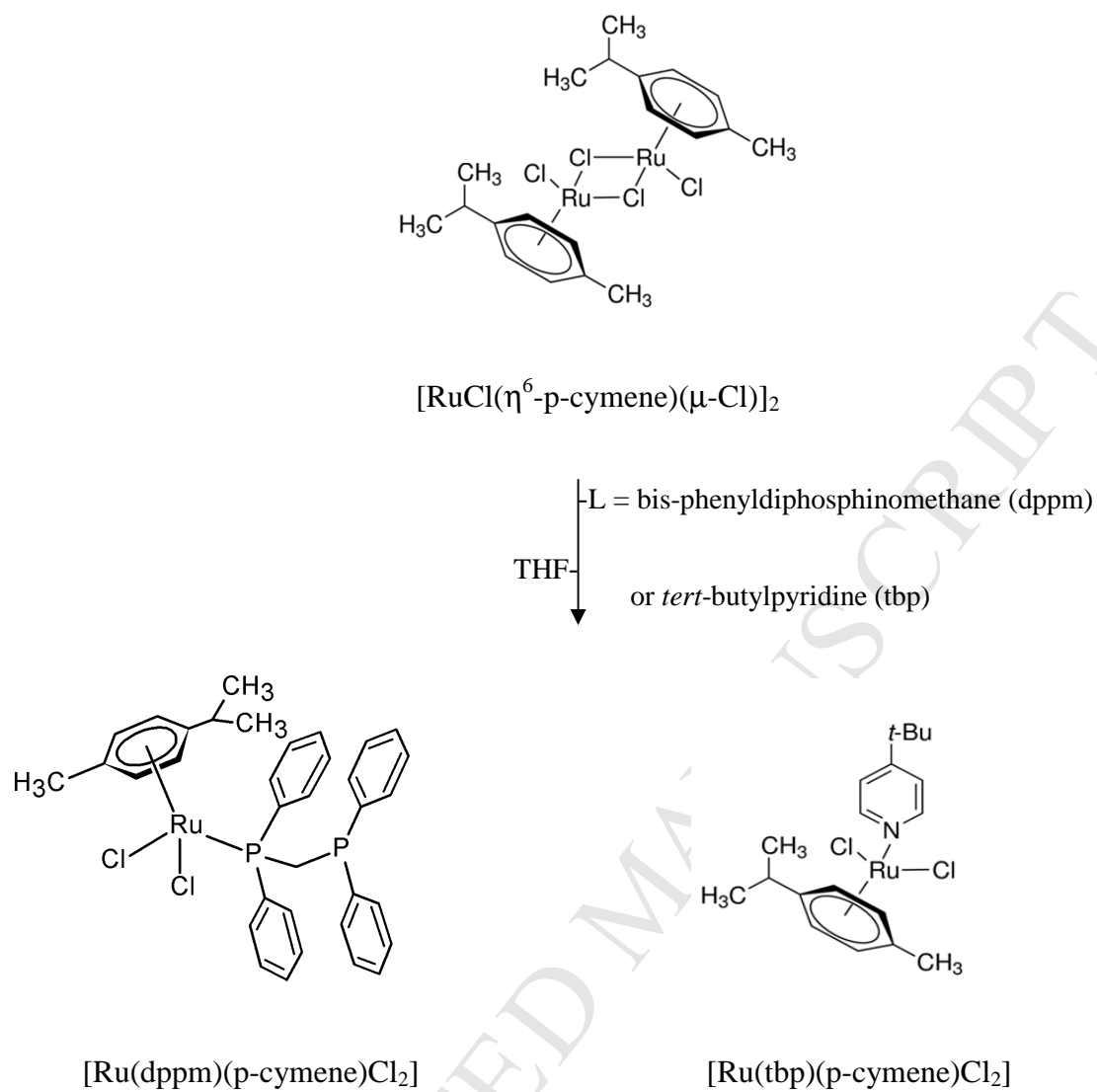
Compounds	Bacteria (µg/mL)						Yeast (µg/mL)	
	SA		MRSA		EC		CN90113	
	MIC	MBC	MIC	MBC	MIC	MBC	MIC	MFC
[Ru(dppm)(pcymene)Cl ₂]	8	200	32	128	NA	NA	64	128
[Ru(tbp)(p-cymene)Cl ₂]	NA	NA	NA	NA	NA	NA	NA	NA
[[RuCl((p-cymene))(µ-Cl)] ₂]	NA	NA	NA	NA	NA	NA	NA	NA
dppm	NA	NA	NA	NA	NA	NA	NA	NA
tbp	0.5	NA	NA	NA	NA	NA	NA	NA
Vancomycin	-	1	1	2	-	-	-	-
Gentamicin	-	1	1	-	0.5	-	-	-
Amphotericin B	-	-	-	-	-	-	0.25	0.5

SA = *Staphylococcus aureus* ATCC25923, MRSA = methicillin - resistant *Staphylococcus aureus*, *Escherichia coli* ATCC25922, CN90113 = *Cryptococcus neoformans* ATCC90113 flucytosine - resistant MIC = minimum inhibitory concentration (µg/mL), MBC= minimum bactericidal concentration (µg/mL), MFC= minimum fungicidal concentration (µg/mL), NA = non active

Table 3. IC₅₀ mean values (μM) for [Ru(p-cymene)(dppm)Cl₂], [Ru(p-cymene)(tbp)Cl₂], and cisplatin against MCF-7 and HCC1937 cells after 48 h of treatment. (All data are the mean and standard errors obtained from four independent experiments, each performed in at least triplicate)

Metal complexes	IC ₅₀ (μM)	
	MCF-7	HCC1937
Cisplatin ^[29]	42.2 ± 8 ^{*,**}	23.4 ± 7 ^{*,**}
[Ru(p-cymene)(dppm)Cl ₂]	2.6 ± 0.2 ^{*,**}	1.4 ± 0.3 ^{*,**}
[Ru(p-cymene)(tbp)Cl ₂]	642.6 ± 6.6 ^{*,**}	385.1 ± 5.3 ^{*,**}

Statistical significance differences are indicated by ^{*}*p*<0.01, compared to the IC₅₀ values of the same complex on cell lines, and ^{**}*p*<0.001, compared to the IC₅₀ values of the complexes on each cell line.



Scheme I. Synthesis of the $[\text{Ru}(\text{dppm})(\text{p-cymene})\text{Cl}_2]$ and $[\text{Ru}(\text{tbp})(\text{p-cymene})\text{Cl}_2]$ complexes.

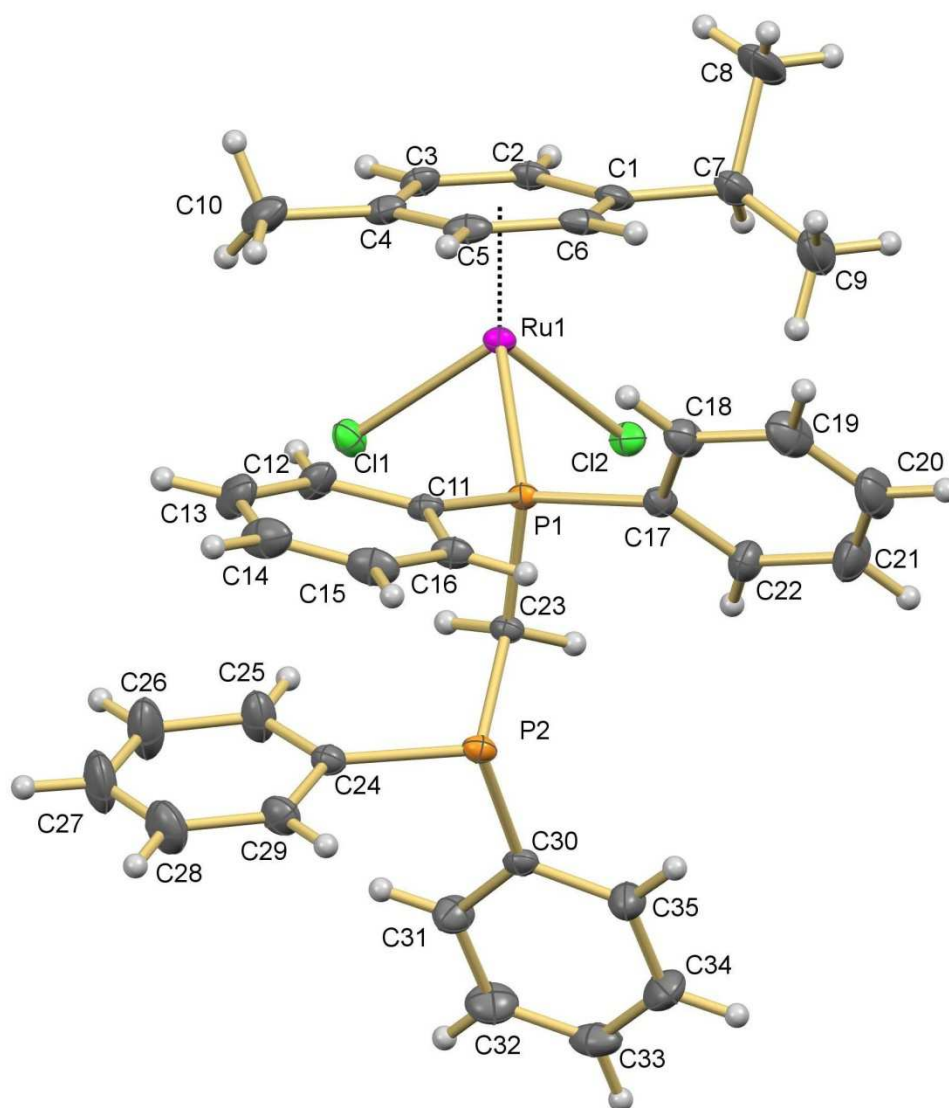


Figure 1. An ORTEP structure of [Ru(p-cymene)(dppm)Cl₂] complex with atom numbering

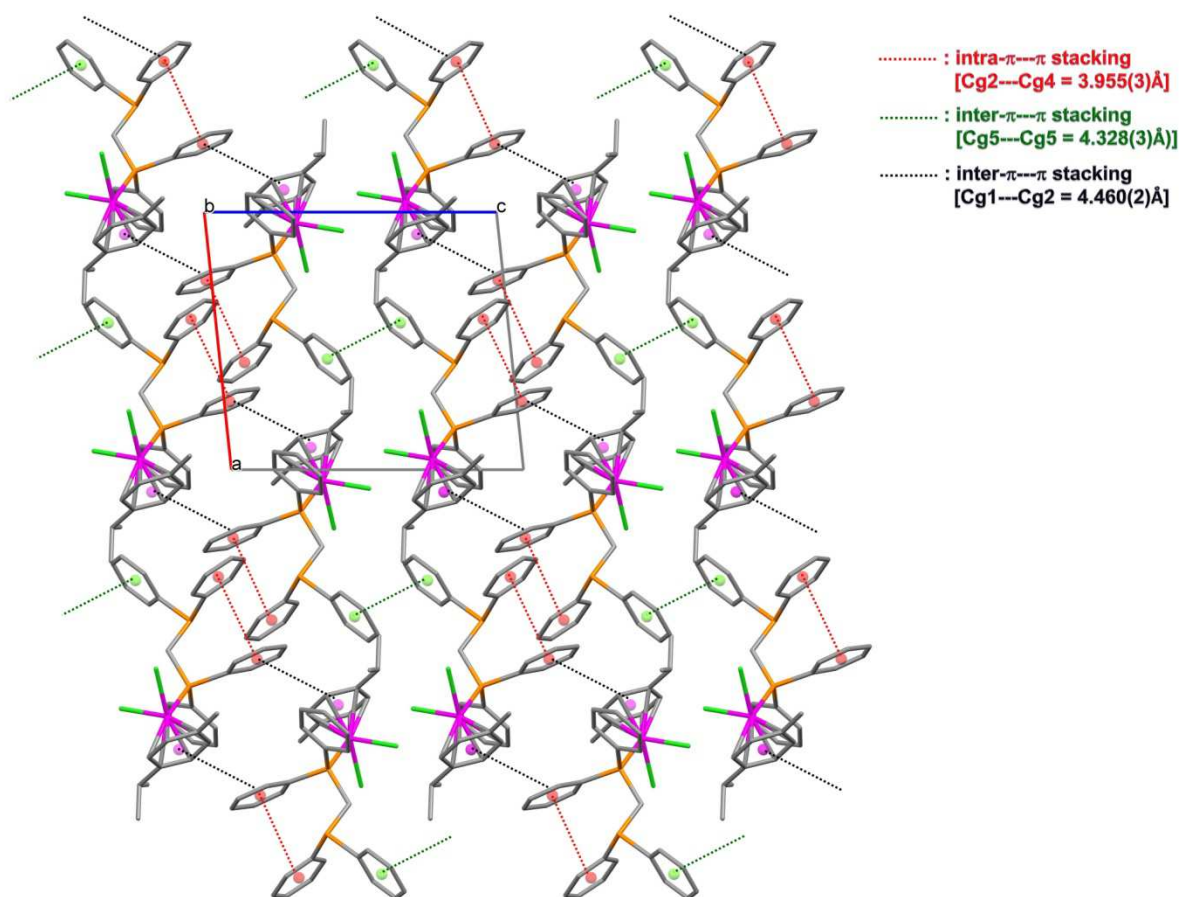


Figure 2. The packing interactions of [Ru(p-cymene)(dppm)Cl₂] complex

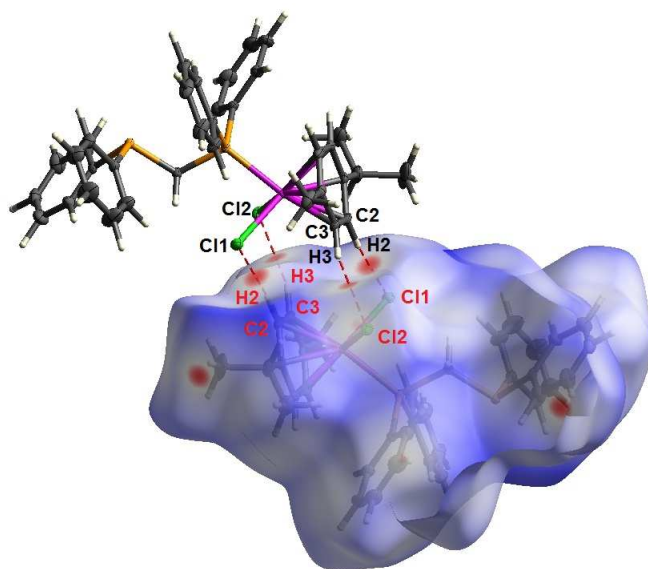


Figure 3. Hirshfeld surface analysis mapped for [Ru(p-cymene)(dppm)Cl₂] complex over *d* norms showing hydrogen bonds of C-H...Cl with neighboring molecules.

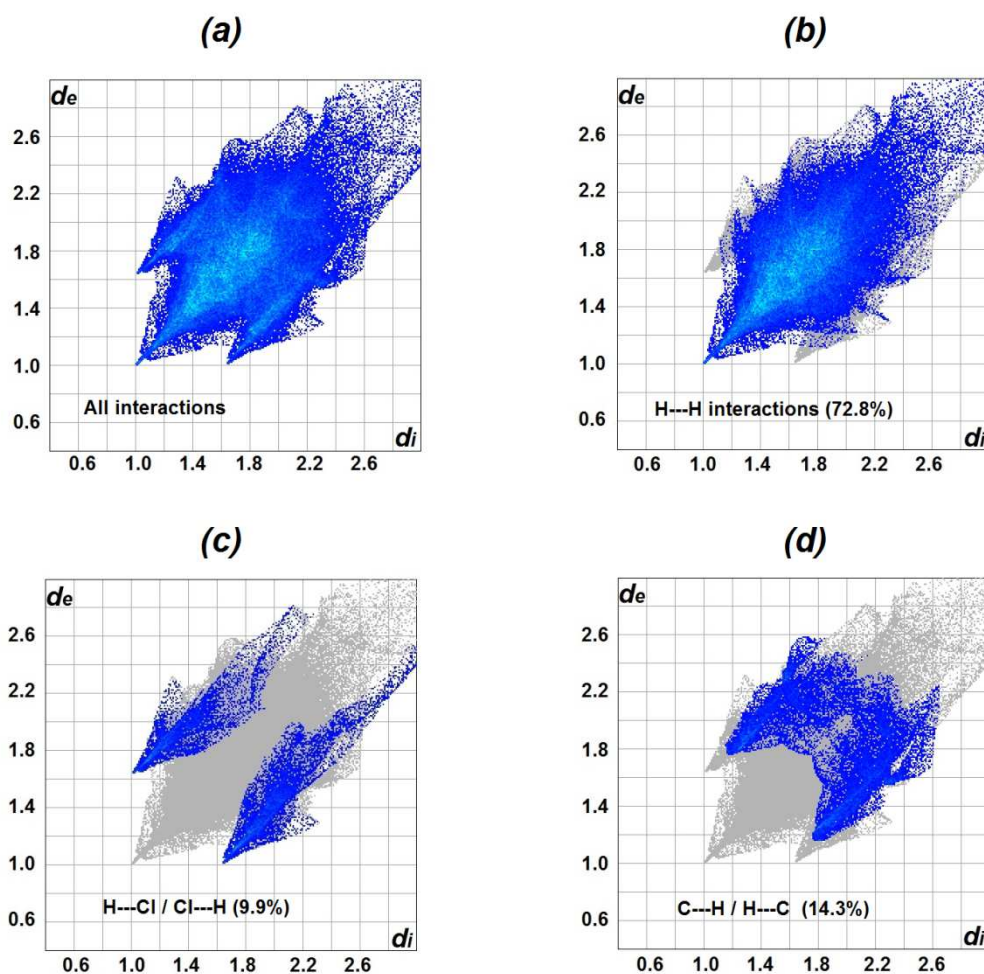


Figure 4. Two-dimensional fingerprint plots of $[\text{Ru}(\text{p-cymene})(\text{dppm})\text{Cl}_2]$ complex: (a) overall interactions and pictured into contributions from different contacts, (b) H---H , (c) H---Cl/Cl---H and (d) C---H / H---C, respectively.

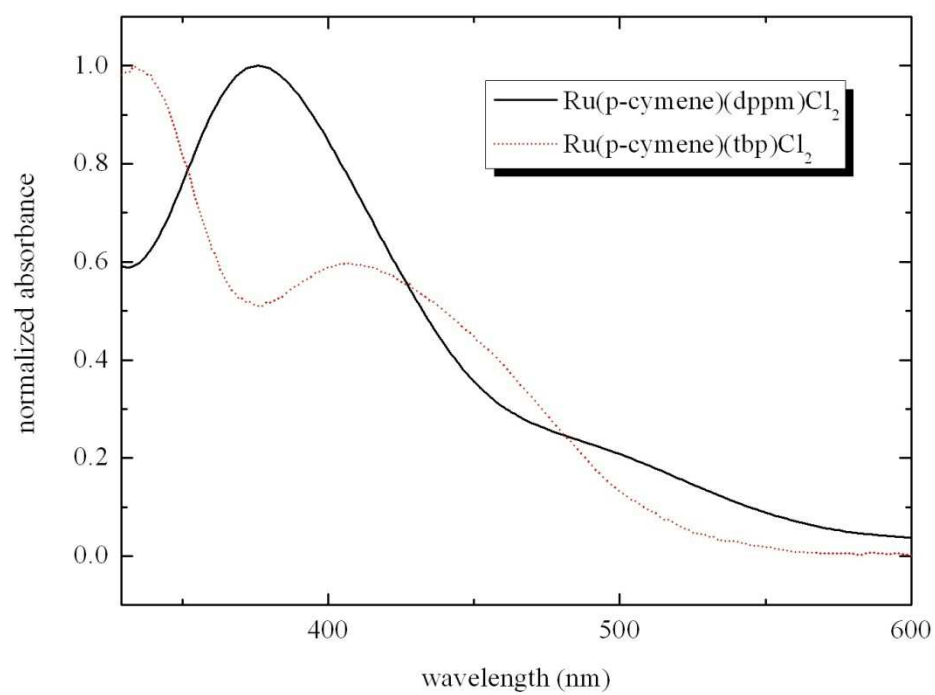


Figure 5 Normalized absorption spectra of $[\text{Ru}(\text{p-cymene})(\text{dppm})\text{Cl}_2]$ and $[\text{Ru}(\text{p-cymene})(\text{tbp})\text{Cl}_2]$

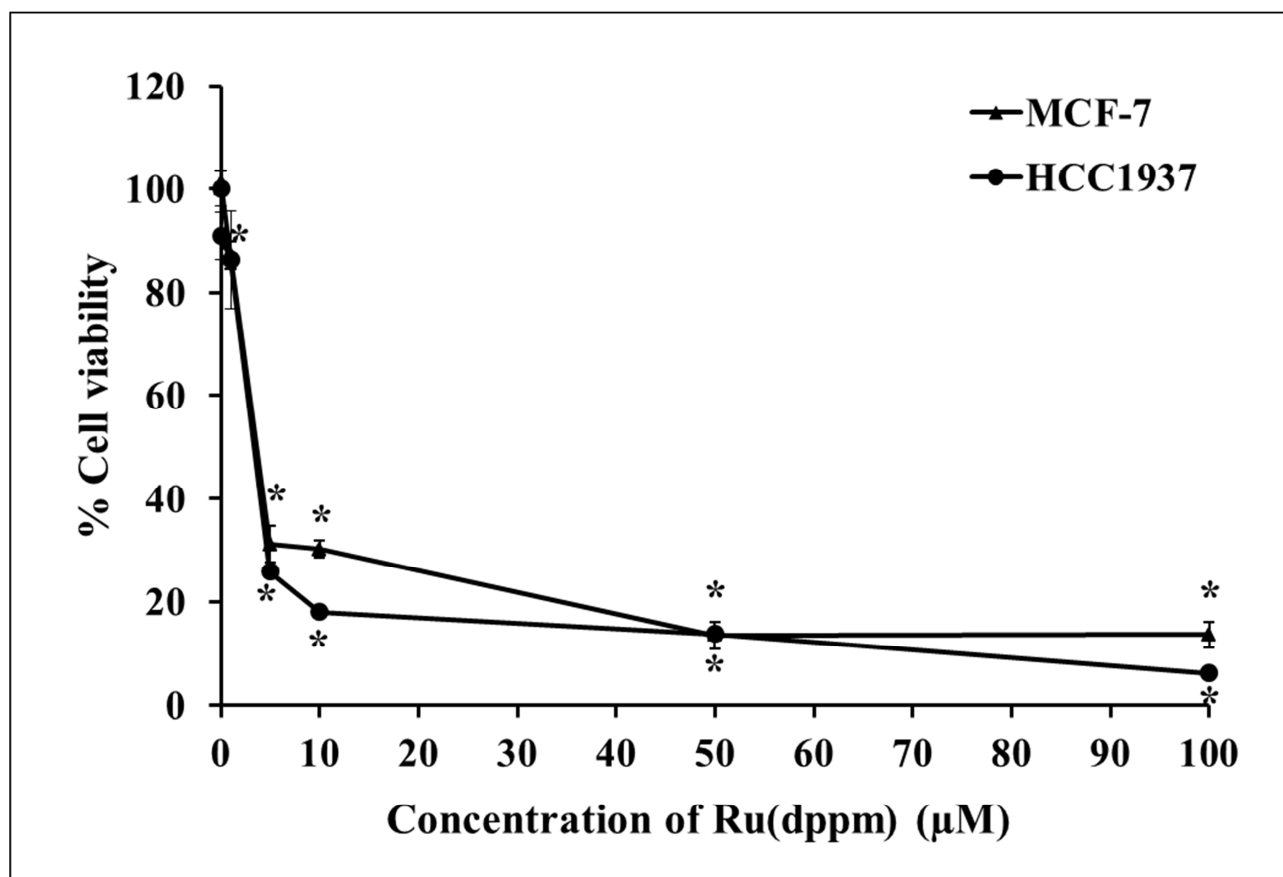


Figure 6. Antiproliferative effect of [Ru(p-cymene)(dppm)Cl₂] on human breast cancer cells using the MTT assay. MCF-7 and HCC1937 cells were treated with various concentrations of [Ru(p-cymene)(dppm)Cl₂] at 37°C in 5% CO₂ for 48 h. Each result point was the percentage of cell viability mean values ± standard error obtained from four independent experiments.

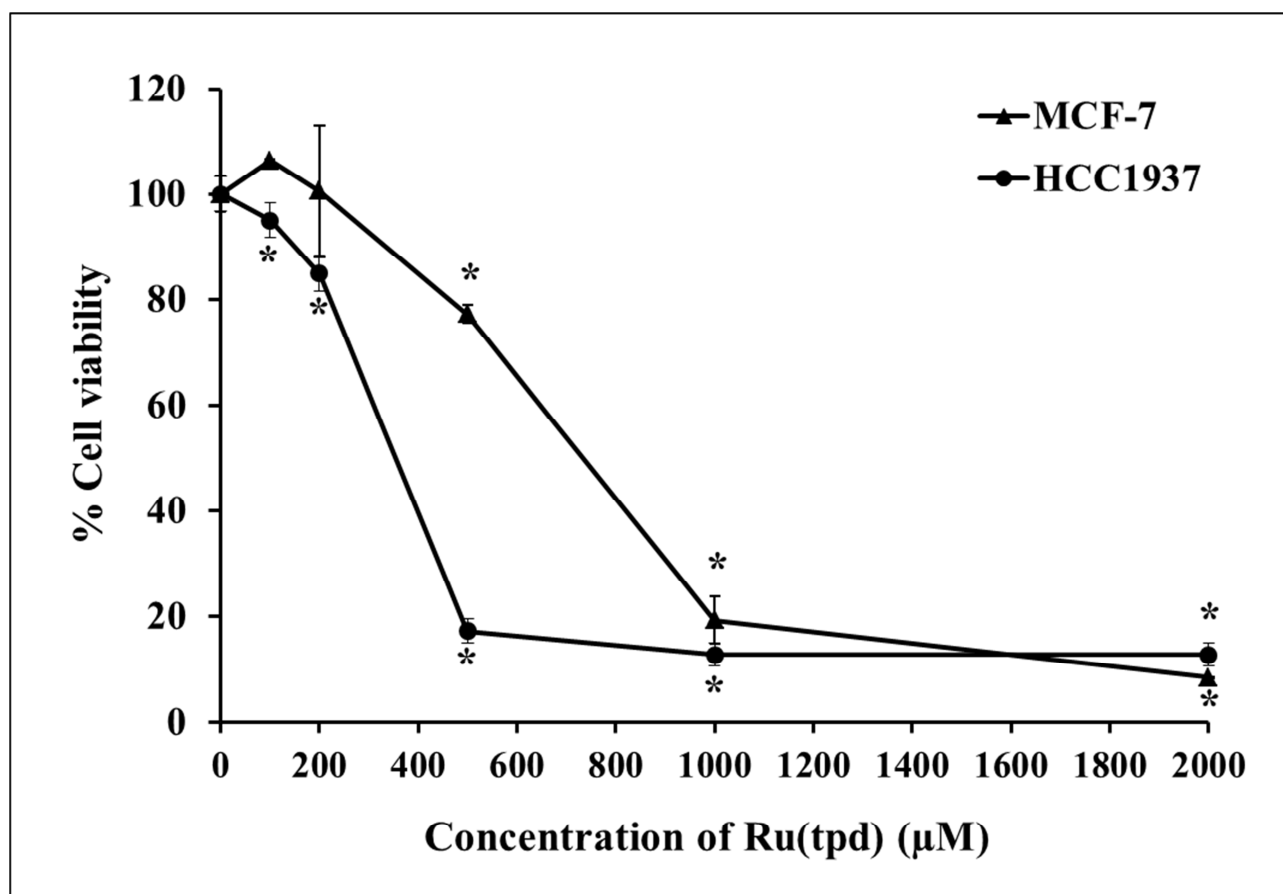


Figure 7. Antiproliferative effect of [Ru(p-cymene)(tbp)Cl₂] on human breast cancer cells using the MTT assay. MCF-7 and HCC1937 cells were treated with various concentrations of [Ru(p-cymene)(tbp)Cl₂] at 37°C in 5% CO₂ for 48 h. Each result point was the percentage of cell viability mean values ± standard error obtained from four independent experiments.

Highlight for review

Synthesis, X-ray structure of organometallic ruthenium (II) p-cymene complexes based on P- and N- donor ligands and their in vitro antibacterial and anticancer studies

Various organometallic (η^6 -arene)-ruthenium (II) complexes with half sandwich of *p*-cymene ligand offer a promising behavior of medicinal applications like anticancers and antibacterial activities. The monodentate bonding of 1,1-bis(diphenylphosphino)methane (dppm) to ruthenium(II) complex in the model of $[\text{Ru}(\text{p-cymene})(\text{dppm})\text{Cl}_2]$ was synthesized. It showed the biological activities of the growth inhibition of breast cancer cell lines (MCF-7 and HCC1937) with satisfied IC_{50} values which are lower than that of cisplatin drug for over 16-folds. The result was also compared to the complex of $[\text{Ru}(\text{p-cymene})(\text{tbp})\text{Cl}_2]$; *tbp* = *tert*-butylpyridine. It was found that the pyridine complex showed much lower activity than it is with the diphosphino complex. In addition, the complex of $[\text{Ru}(\text{p-cymene})(\text{dppm})\text{Cl}_2]$ significantly inhibited *Staphylococcus aureus* ATCC25923, *MRSA* = *methicillin* - resistant *Staphylococcus aureus* with MIC/MBC values of 8/200 and 32/128 $\mu\text{g. mL}^{-1}$, respectively while the $[\text{Ru}(\text{p-cymene})(\text{tbp})\text{Cl}_2]$ complex showed none of inhibition.